

MOL #90092

**ATF3 protects against pressure overload heart failure via autophagy molecule
beclin-1 pathway**

Heng Lin, Hsiao-Fen Li, Hsi-Hsien Chen, Pei-Fang Lai, Shu-Hui-Juan, Jin-Jer Chen,
and Ching-Feng Cheng

Department of Physiology, School of Medicine, College of Medicine, Taipei Medical University, Taipei, Taiwan (H.L., H.-F.L., S.-H.J); Institute of Biomedical Sciences, Academia Sinica, Taipei, Taiwan (C.-F.C.); Division of Nephrology, Department of Internal Medicine, Taipei Medical University Hospital, Taipei, Taiwan (H.-H.C.); Department of Internal Medicine, School of Medicine, College of Medicine, Taipei Medical University, Taipei, Taiwan (H.-H.C.); Department of Emergency Medicine, Tzu Chi General Hospital, Hualien, Taiwan (P.-F.L.); Department of Internal Medicine and Graduate Institute of Clinical Medical Science, China Medical University, Taichung, Taiwan (J.-J.C.); Department of Medical Research, Tzu Chi General Hospital and Department of Pediatrics, Tzu Chi University, Hualien, Taiwan (C.-F.C.).

MOL #90092

Running title: ATF3 regulates cardiac hypertrophy

Correspondence: Dr. Ching-Feng Cheng, Department of Medical Research, Tzu Chi General Hospital, Hualien, Taiwan. E-mail:chengcf@mail.tcu.edu.tw; Tel: 886-3-8561825 ext:5629; and Dr. Jin-Jer Chen, Department of Internal Medicine and Graduate Institute of Clinical Medical Science, China Medical University, Taichung, Taiwan. E-mail: jc8510@yahoo.com.

Number of:

Text pages: 44

Table: 1

Figure: 6

Reference: 45

Words in Abstract: 241

Words in Introduction: 414

Words in Discussion: 1413

Abbreviations: ATF3, activating transcription factor 3; AAV, adeno-associated virus; ChIP, chromatin immune-precipitation; CREM, cAMP response element modulator; LV, left ventricle; TAB, transverse aortic banding; tBHQ, tert-butylhydroquinone; TUNEL, TdT-mediated dUTP-biotin nick end labeling.

MOL #90092

Abstract

Activating transcription factor 3 (ATF3), a CREB/ATF family transcription factors member, has been implicated in cardiovascular and inflammatory system and is rapidly induced by ischemic-reperfusion injuries. We performed transverse aortic banding (TAB) experiments using ATF3 gene-deleted mice (ATF3^{-/-}) and wild-type (WT) mice to find out what effect it may have on heart failure induced by pressure overloading. Compared to the WT mice, ATF3^{-/-} mice were found by echocardiography to have decreased left ventricular contractility with loss of normal cardiac hypertrophic remodeling. The ATF3^{-/-} mice had greater numbers of TUNEL-positive cells and higher levels of activated caspase-3 as well as more apoptosis. Restoration of ATF3 expression in the heart of ATF3^{-/-} mice by adenovirus-induced ATF3 treatment significantly improved cardiac contractility following TAB. The results from molecular and biochemical analyses, including chromatin immune-precipitation (ChIP) and in vitro /in vivo promoter assays, showed that ATF3 bound to the ATF/CRE element of the beclin-1 promoter and that ATF3 reduced autophagy via suppression of the beclin-1 dependent pathway. Furthermore, infusion of tert-butylhydroquinone (tBHQ), a selective ATF3 inducer, increased the expression of ATF3 via the NRF2 transcriptional factor, inhibited TAB-induced cardiac dilatation, and increased left ventricular contractility, thereby rescuing heart

MOL #90092

failure. Our study identified a new epigenetic regulation mediated by the stress-inducible gene ATF3 on TAB-induced cardiac dysfunction. These findings suggest that the ATF3 activator tBHQ may have therapeutic potential for the treatment of pressure overload heart failure induced by chronic hypertension or other pressure overload mechanisms.

Introduction

In response to stress from neurohumoral activation, hypertension, or other myocardial injuries, the heart initially compensates with an adaptive hypertrophic response such as autophagy and transcriptional factor activation, which increases cardiac mass. Under prolonged stress, however, the heart undergoes irreversible changes, resulting in chamber dilatation and diminished heart performance (Feihl et al., 2008). Autophagy can be induced by starvation, hypoxia, intracellular stress, hormones, or developmental signals (Klionsky et al., 2000; Levine et al., 2004). Autophagy, which can be defined as a self-eating process, is a mechanism through which cells degrade their own components and recycle amino acids and other building blocks that can eventually be reused (Yorimitsu et al., 2005). Depending on which pathway through which cellular components are delivered to lysosomes, three types of autophagy can be distinguished--macroautophagy, microautophagy, and chaperone-mediated autophagy (Dutta et al., 2012). Macroautophagy, which primarily occurs in the heart, may be either beneficial or deleterious under pressure overload conditions, depending on the circumstances under which it is induced, the extent to which it is stimulated, and the signaling pathways that are activated (Zhu et al., 2007; Cao et al., 2011).

MOL #90092

Activating transcription factor 3 (ATF3), a member of the CREB/ATF family of transcription factors (Chen et al., 1994), is rapidly induced by ischemic-reperfusion injuries in the heart or kidney (Chen et al., 1996; Li et al., 2010). ATF3 can repress or activate target genes by forming homo- or heteromeric complexes (Hsu et al., 1992). Heart of alpha-myosin heavy chain-driven ATF3 transgenic mice have been observed to have atrial enlargement and as well as atrial and ventricular hypertrophy accompanied with reduced contractility and aberrant conduction (Okamoto et al., 2001). Although autophagy is known to play an important role in the adaptive hypertrophic response in the heart, it is unclear whether ATF3 is involved in pressure overload-induced cardiac remodeling or heart failure.

In the present study, ATF3 gene-deleted (ATF3^{-/-}) mice were found to have loss of normal hypertrophic remodeling in response to trans-aortic banding (TAB) with early pressure overload-induced heart failure. Beclin-1, the mammalian homolog of a pro-autophagic gene, was found to be targeted by ATF3. ATF3 re-expression by adeno-associated virus (AAV) infection in ATF3^{-/-} mice or supplementation with the ATF3-specific inducer tBHQ reduced the progression of pressure overload-induced heart failure in TAB mice. These findings suggest that ATF3 plays a crucial role in hypertrophic cardiac remodeling and that an ATF3 analogue or inducer may

MOL #90092

potentially be used in the treatment of patients with chronic high blood pressure diseases.

Materials and Methods

Animal model for cardiac transverse aortic banding (TAB) and tBHQ injection

The ATF3^{-/-} mice were kindly provided by Dr. Tsonwin Hai (Ohio State University, OH, USA). The ATF3^{-/-} allele was backcrossed into C57BL/6 mice for at least seven generations before cardiac TAB procedure. Male mice (weighing 25–30 g) were anesthetized with intra-peritoneal (i.p.) injection of chloral hydrate (125 mg/kg). TAB procedure was performed as prior description (Hu et al., 2003). tBHQ therapy was performed at fourth week after TAB or sham surgery. Mice were given i.p. injections of 1 mg/kg/week tBHQ (Sigma-Aldrich Co., St. Louis, MO, U.S.A.) for 7 weeks. The control group was treated with 0.1 ml saline (instead of tBHQ) for 7 weeks. Echocardiography was performed at the fourth and tenth week after TAB or sham surgery. After therapy, the mice were sacrificed by overdose sodium pentobarbital (200 mg/kg, i.p.) and the hearts were rapidly excised for further experiments. All surgical procedures were performed according to the protocols approved by the Institutional Animal Care and Utilization Committee, Academia Sinica, Taipei, Taiwan.

Cell culture

MOL #90092

Cardiomyocytes cell line (H9c2), human embryonic kidney (HEK 293) cells and kidney epithelial cell line (NRK-52E cells) were maintained in Dulbecco's modified Eagle's medium supplemented with 10% FBS, 100 U/ml penicillin, and 100 µg/ml streptomycin.

Cytoplasmic and nuclear protein extraction

Cells and heart tissues were separated into cytoplasmic and nuclear parts using a ProteoJET™ protein extraction kit (Fermentas Life Sciences, MA, U.S.A.).

Western blot analysis

Extracts of heart and cells were separated on an SDS-PAGE and subjected to western blot analysis using the protocol of ECL kit (Pierce, Ill, U.S.A.). Antibodies, including the following: anti-ATF3 (1:500, Santa Cruz, CA, U.S.A.), anti-Lamin A/C (1:1000, GeneTex, CA, U.S.A.), anti-Becn1 (1:1000, Santa Cruz), anti-GAPDH (1:10000, BD Pharmingen, NJ, U.S.A.), anti-caspase 3 (1:1000, Cell Signaling, MA, U.S.A.), and anti-β-actin (1:10000, Millipore, Darmstadt, Germany), and anti-LC3B (1:500, Cell Signaling, MA, U.S.A.) were used.

Immunohistochemistry

MOL #90092

Tissue slides were de-waxed and then treated with epitope retrieval buffer (Thermal Scientific, Inc., Texas, U.S.A.) in 95° for 30 min. Then slides were quenched with 3% H₂O₂, blocked by Power Block™ (Biogenex, CA, U.S.A.), and incubated for 10 min at room temperature. The sections were then incubated with rabbit anti-ATF3 (1:100, Santa Cruz) for 18 hrs at 4°C and washed for 5 times with PBS-T. Anti-rabbit antibody (biotinylated, 1:200, Vectastain kit, Vector Labs, CA, U.S.A.) were applied to slides for 1 hr at room temperature. Then slides were incubated with ABC reagent (Vectastain kit) at room temperature for 30 min and washed twice with PBS-T. The nuclei were stained with DAB (Vectastain kit) for microscopic studies.

Real-time quantitative PCR and reverse transcription (RT)-PCR

Total RNA was extracted from the heart using Trizol (Invitrogen, CA, U.S.A.). Real-time quantitative PCR analysis was performed using the ABI PRISM 7700 Sequence Detection System (Applied Biosystems, NY, U.S.A.). For RT-PCR, total RNA was extracted from the heart using Trizol. cDNA was prepared with the Super Script kit (Invitrogen) from 3µg of total RNA with Oligo (dT) for analysis. Primers used are listed in Table 1.

***In vitro* protein synthesis and electrophoretic mobility shift assay (EMSA)**

MOL #90092

For EMSA assay, the *in vitro* translated ATF3 was performed using the T7 polymerase-based TNT quick coupled transcription/translation kit (Promega, WI, U.S.A.) and then incubated with the beclin-1 DNA probes containing a consensus ATF3 binding site. Probes used are listed in Table 1. EMSA analysis was performed as described previously (Lin et al., 2008). Briefly, the binding reactions were performed in 20- μ L reaction mixtures with the *in vitro* translated products. Reactions were loaded on a 5% polyacrylamide gel and run at 100 V at 4°C in 0.5x TBE. The gel was dried and exposed to a phosphorimager screen (Molecular Dynamics, Ill, U.S.A.).

Chromatin immunoprecipitation (ChIP) assay

After Adenovirus infection, H9c2 cells were fixed in 1 % formaldehyde and ChIP assay was performed using the Upstate protocol (Millipore). Chromatin was immunoprecipitated using anti-ATF3 antibody (Santa Cruz). The purified DNA was detected using standard PCR. Primers used are listed in Table 1.

***In Vitro* promoter assay**

For *in vitro* promoter assay, ATF/CRE binding site from the Beclin-1 promoter (-1~-1.4kb) were inserted into upstream of the luciferase reporter in pGL-4 vector

MOL #90092

(Promega) to create pGL4-beclin-1. NRK-52E cells were transfected with or without pGL4-beclin-1 and pcDNA3-ATF3 for 24 hrs before harvesting for luciferase assay. Firefly luciferase activity was determined and normalized to Renilla luciferase activity. Data shown represent averages and SEM acquired from three independent experiments.

Echocardiography studies

For echocardiography, mice were anesthetized with phenobarbital (40 mg/kg body weight, i.p.) and then measurements were taken with an ultrasound equipment (ATL Philips IE33, Ultrasound Machine System, CA, U.S.A.) using a 15-MHz probe. The left ventricular posterior wall thickness (LVPW), inter-ventricular septum thickness (IVS), and left ventricular lumen diameter at both end-systolic and end-diastolic phases were measured digitally on the M-mode tracings and averaged for three cardiac cycles. Fractional shortening (FS) and ejection fraction (EF) were then calculated.

Histology

Heart from all the treated groups were fixed in 4% paraformaldehyde for overnight at 4°C and processed with paraffin fixation. Sections (5 µm) were stained with

MOL #90092

hemotoxylin & eosin and Masson's trichrome.

Myocardial injection of plasmid DNA

C57/B6 and ATF3^{-/-} mice were anesthetized with phenobarbital (40 mg/kg body weight, i.p.) and subsequently intubated with an 18-gauge angiocath and mechanically ventilated (model-697 ventilator; Harvard Apparatus, Holliston, MA, U.S.A.). Body temperature was maintained at 37°C with a heating pad plus a heating lamp. A midline sternotomy was performed under sterile technique. Then 5 µg plasmid DNA in 30 µL PBS or the same volume of PBS alone was injected into the anteriolateral wall of the left ventricle using a 30-gauge needle. Plasmid DNA containing a promoterless Fluc (pGL4-basic vector) as a negative control, or pGL4-beclin-1 was injected. Firefly luciferase activity was determined and normalized to Renilla luciferase activity. Data shown represent averages and SEM from three independent experiments was done in triplicate each.

TdT-mediated dUTP-biotin nick end labeling (TUNEL) assay

Mice were perfused with 4% paraformaldehyde in 0.1M phosphate buffer (pH 7.4) and hearts were dissected and fixed in 4% paraformaldehyde overnight at 4°C, embedded in paraffin, and sectioned (5 µm). Apoptosis in heart tissues was identified

MOL #90092

by TUNEL assay with an *in situ* Cell Death Detection kit (Roche Applied Science, Indianapolis, IN, U.S.A.) following the manufacturer's instructions.

Production of recombinant adeno-associated virus carrying ATF3

Full-length ATF3 was obtained by polymerase chain reaction (PCR) amplification from a human complementary cDNA library, flanking the XbaI and HindIII restriction cutting sites, and was cloned into the pAAV-MCS vector. To produce the AAV virus, a three-plasmid co-transfection method was used (Xiao et al., 1998). The plasmids used in transfection were as follows: (i) the AAV-CMV-ATF3 plasmid with the gene driven by the CMV promoter, which carried the promoter-driven transgene flanked by AAV inverted terminal repeats; (ii) the helper plasmid, which contained helper genes from the adenovirus; and (iii) the pseudotyped AAV packaging plasmid containing the AAV8 serotype capsid gene coupled with the AAV2 rep gene. The wild-type of AAV (the control) or AAV-ATF3 (the experimental group) was purified two times by CsCl gradient ultracentrifugation, and the titer of vector genome particles was determined using a previously described method (Rabinowitz et al., 2002). The recombinant viruses with 1×10^{12} viral particles in 30 μ l of PBS were injected into a mouse tail vein 2 weeks after TAB treatment.

MOL #90092

Statistical analysis

Data are expressed as mean \pm SEM. Differences between groups were analyzed by unpaired Student's t-test. $P < 0.05$ was considered statistically significant.

Results

Increased ATF3 expression with transient nuclear translocation was observed in murine cardiac hypertrophic remodeling induced by trans-aortic banding

Initially, we intended to confirm that ATF3 played a role in the cardiac hypertrophic remodeling induced by TAB in mice. Twenty-four hours after TAB, we observed an approximately 4-fold increase in the cardiac ATF3 mRNA levels in the study mice, compared to the controls. This enhanced expression of ATF3 persisted for seven days following TAB (Fig. 1A). Immuno-histochemical data and western blot analysis from LV tissue showed that nuclear expression of ATF3 was highest at 1 day after TAB, with cytosolic expression of ATF3 highest at day 3-7 after TAB (Fig. 1B and Fig. 1C). At the same time, however, the expressions of myocardial ATF3 mRNA and cytosolic ATF3 protein remained elevated (Fig. 1A and 1B).

ATF3^{-/-} mice showed loss of normal cardiac hypertrophic remodeling with early pressure overload heart failure

MOL #90092

Because TAB-induced cardiac hypertrophy is frequently accompanied by re-expression of the cardiac fetal genes, we examined the expression of atrial natriuretic factor (ANF), brain natriuretic peptide (BNP), α -myosin heavy chain (α -MHC), and β -myosin heavy chain (β -MHC) in the banded WT and ATF3^{-/-} hearts using real-time quantitative PCR. The expression levels of ANF, BNP, and β -MHC were significantly increased in the heart of banded ATF3^{-/-} mice compared with that of WT mice, with no difference in α -MHC expression levels (Fig. 2A). Echocardiographic data showed that LV ejection fraction and fractional shortening decreased significantly with chamber dilatation in the ATF3^{-/-} mice one week after TAB treatment compared with WT mice (Supplementary Fig. 1). Moreover, histological examination showed significant fibrosis without normal hypertrophic remodeling after TAB in the LV of ATF3^{-/-} mice compared with that of WT mice (Fig. 2B). We also observed increased numbers of apoptotic cells with TUNEL-positive staining (Fig. 2C) and increased expression of active form of caspase-3 expression in the ATF3^{-/-} mice compared with WT mice after TAB treatment (Fig. 2D). Together, our findings suggest that ATF3 plays an important protective role in pressure overload cardiac remodeling induced by TAB.

Restoration of ATF3 expression rescued TAB-induced pressure overload heart

failure in the ATF3^{-/-} mice

As a complementary approach to our knockout mouse studies, we performed phenotype rescue studies in which ATF3^{-/-} mice received AAV8-mediated gene transfer of ATF3 (AAV8-ATF3) (Wang et al., 2005). Three weeks after AAV8-ATF3 i.v. injection, the expression of ATF3 in the hearts of ATF3^{-/-} mice was significantly increased (Fig. 3A), LV contractility was recovered (Fig. 3B) and chamber dilatation was attenuated (see Supplementary Fig. 2). In addition, TAB-induced cardiac fibrosis was attenuated in the ATF3^{-/-} mice after *in vivo* AAV8-ATF3 therapy (Fig. 3C). Taken together, our results suggest that ATF3 is a key regulator of TAB-induced cardiac remodeling and heart failure.

Inhibition of beclin-1 activity by ATF3

Because the presence of the ATF3 binding sites ATF/CRE on the promoter region of beclin-1 can up-regulate beclin-1 via ROS-mediated ischemic-reperfusion injury in the heart (Ma et al., 2012), it is possible that increased ATF3 during cardiac hypertrophic remodeling may be regulated through beclin-1 signaling. To test this hypothesis, we first examined whether the expression of beclin-1 could be regulated

MOL #90092

by ATF3 in cardiomyocytes (H9c2) cells. As shown in Figure 4A, beclin-1 expression was high in the HPGK vector infected H9c2 cells under both normal and starved conditions, whereas its expression was decreased in ATF3 vector infected H9c2 cells under starvation conditions, suggesting that ATF3 might down-regulate beclin-1 expression following stress. Consistent with the above results, under either sham operated condition or 3 days after TAB procedures, the stress induced by TAB was found to induce beclin-1 expression in both ATF3^{-/-} and WT mice, with higher beclin-1 and LC3II levels observed in the ATF3^{-/-} mice compared with the WT group (Fig. 4B and Fig. 4C).

To further identify whether the regulation of beclin-1 expression by ATF3 was dependent on the translocation/binding of ATF3 to the ATF/CRE element, we performed an EMSA DNA-binding assay using ATF/CRE binding sequence located in the beclin-1 promoter (-164 to -156bp and -182 to -175bp) from mouse DNA. ATF3 DNA-binding activity was observed in the nuclear extracts, but this activity was markedly suppressed in cells pretreated with unlabeled cold primer (Fig. 4D lane 5 vs. lane 6). Furthermore, gel retardation was abolished by ATF3 antibody when this antibody blocked the DNA binding domain of ATF3 (Fig. 4D, lane 5 vs. lane 7). A ChIP assay was conducted to further examine whether ATF3 was located in the

MOL #90092

nucleus and whether it could bind to the ATF/CRE element of the beclin-1 promoter. The adenovirus-ATF3 (Adv-ATF3) infected H9c2 cells presented a higher binding activity on the ATF/CRE element than the Adv-HPGK control cells (Fig. 4E).

To further substantiate the binding activity of ATF3 on the ATF/CRE binding region of beclin-1, luciferase assay was performed in NRK-52E cells. When luciferase expression vectors were transfected with mouse beclin-1 promoter plasmid, the addition of ATF3 significantly suppressed beclin-1 luciferase activity (Fig. 4F, lane 2 vs. lane 3). The inhibition of beclin-1 luciferase activity by ATF3 was also observed under starvation conditions in these cells (Fig. 4G, lane 5 vs. lane 6). Finally, to characterize whether ATF3 could suppress beclin-1 transcriptional expression *in vivo*, we used methods suggested by a prior study (von Harsdorf et al., 1997) to inject luciferase-containing-beclin-1 promoter plasmid into the hearts of both WT and ATF3^{-/-} mice. Increased luciferase activity was observed after the pGL4-beclin-1 promoter injection in the wild type mice (Fig. 4G) and decreased activity was observed 3 days after TAB treatment (Fig. 4G, lane 2 vs. lane 4). However, the luciferase activity was significantly higher in the ATF3^{-/-} mice after TAB treatment compared with the former group (Fig. 4G, lane 4 vs. lane 6). Together, our findings suggest that ATF3 can repress beclin-1 protein level via transcriptional regulation in

vivo.

An ATF3 specific inducer, tBHQ, can attenuate TAB-induced pressure overload heart failure in mice

Prior studies have reported that tBHQ, an ATF3-specific inducer, can inhibit cell death or exert an anti-inflammatory effect (Kim et al., 2010; Hoetzenecker et al., 2011). Therefore, we were interested in elucidating the role of tBHQ in protecting against TAB-induced heart failure in mice. Initially, using varying doses of tBHQ in the administration of single injections, we found a 4- to 6-fold increase in cardiac ATF3 expression at days 1 and 7 after injection (Fig. 5A). Although the higher doses appeared more effective in ATF3 induction, there was no positive correlation between the dosage and cardiac ATF3 expression. To minimize possible side effects, we applied (i.p. injection) small doses (1 mg/kg) of tBHQ weekly to TAB mice and evaluated its long-term effect on pressure overload heart failure (experimental design, Fig. 5B). The weekly administrations of tBHQ (1mg/kg) for seven weeks after TAB reduced the LV chamber dilatation and increased LV wall thickness, thus restoring the normal LV contractility (FS: 44% vs. FS: 32%, respectively; $p < 0.01$) compared with the TAB treated group (Fig. 5C). In addition, TAB-induced cardiac apoptosis

MOL #90092

was also attenuated following tBHQ treatment (Fig. 6). These results suggest that the specific ATF3 inducer, tBHQ, could potentially serve as an effective therapeutic molecule to prevent TAB-induced pressure overload heart failure.

Discussion

In this study, TAB-induced pressure overload heart failure with cardiac fibrosis and cells apoptosis was first found to be more severe in the ATF3^{-/-} mice than the WT mice. Re-expression of the ATF3 protein in the heart via a viral infection (AAV-ATF3) was found to ameliorate TAB-induced cardiomyopathy in the ATF3^{-/-} mice through the involvement of the beclin-1-dependent autophagy signaling pathway. Our in vivo experiments demonstrated that by use of the ATF3 specific inducer tBHQ could rescue long-term TAB-induced cardiac dysfunction. Considered together, these results suggest that ATF3 plays a prominent regulatory role in pressure overload-induced heart failure and that supplementation with an ATF3-specific inducer such as tBHQ might potentially be useful in the treatment of future pressure overload-induced cardiomyopathy.

Accumulating evidence has suggested that nuclear transcription factors from the basic leucine zipper (bZIP) family play an important role in cardiac development and function. This bZIP family includes the CREB/ATF family of transcription factors, which include CREB, cAMP response element modulator (CREM), ATF, and the related AP-1 and C/EBP families (Kehat et al., 2006). Our study and a prior study by

MOL #90092

Zhou et al. have shown that ATF3 mRNA levels are up-regulated one day after TAB procedure and loss of the ATF3 gene can aggravate pressure overload-induced cardiomyopathy in mice (Zhou et al., 2011). In addition, we observed that while the nuclear translocation of ATF3 only occurred for a short duration (one day after TAB procedure), ATF3 protein remained continuously generated for at least one week following TAB induction (Figs. 1A and 1B). The ATF3 protein that was continuously presented in the cytoplasm 6 days after TAB may be an alternatively spliced form, an ATF3 delta Zip lacking the leucine zipper domain. ATF3 delta Zip has been found to stimulate transcription, presumably by sequestering inhibitory co-factors (Chen et al., 1994). Although the exact mechanism of how ATF3 delta Zip or cytosolic ATF3 induce cardiac hypertrophy is still unknown, they may modulate gene expression by recruiting ATF4 from the cytosol into the nucleus to affect histone deacetylase (HDAC) activity under stress conditions induced by amino deprivation (Li et al., 2010; St Germain et al., 2010).

ATF3 is transcriptionally upregulated and present in the nucleus at day 1 (Figure 1C) and reduced at day 3-7 after TAB; while beclin-1 increased from day 1 to 3 (Figure 4B) with highest levels on day 3 and declined at day 7 after TAB. The nuclear decrease of ATF3 levels and the increase of beclin1 levels in day 1-3 after TAB

MOL #90092

suggested that ATF3 in the nucleus affected the BECLIN-1 promoter via direct binding and repressed its expression. In addition, ATF3 may have also affected cell autophagy by its localization and interaction with other transcription factors in the cytoplasm. Cardiac hypertrophy can induce ER stress, in that eIF2alpha can be phosphorylated by PEK and induce the expression of ATF4, further upregulating ATF3 and other stress genes (Jiang et al., 2004). ATF4 could promote the transcription of Atg12, resulting in increased autophagy. ER stress can also activate IRE1, leading to subsequent phosphorylation of Bcl2 and prevent its binding to beclin-1, thus activating beclin-1 thereby promoting autophagy (Pattingre et al., 2005; Erlich et al., 2007). Cytoplasmic localization of ATF3 has been reported by others in some breast carcinomas (Wang et al., 2008) and Stat1 knockdown hepatocytes (Kim et al., 2009), though the biological significance of this phenomenon needs further elucidation.

Although signal transduction pathways for cardiac hypertrophy are inherently complex and abundant, studies using animal models have revealed important mediators of cardiac hypertrophy. These mediators can be divided into the following categories: mitogen-activated protein kinase (MAPK) signaling pathway, calcineurin–nuclear factor of activated T cells (NFAT) signaling pathway, insulin-like

MOL #90092

growth factor-I (IGF-I)– phosphatidylinositol 3-kinase (PI3K)– AKT/protein kinase B (PKB)– mammalian target of rapamycin (mTOR) signaling pathway, and ET-1 or angiotensin II-induced calcium-calmodulin-PKC-class II HDACs signaling pathway (Heineke et al., 2006). Our study showed that ATF3 could inhibit both the hypertrophic signaling which is mediated through the MAPK signaling pathway (Fig. 2A) and the ET-1 or angiotensin II associated pathway (see Supplementary Fig. 3), suggesting that ATF3 might also inhibit hypertrophy via the calcium-calmodulin-PKC-class II HDACs signaling pathway. However, it remains unclear whether ATF3 can directly regulate PKC gene regulation (Buganim et al., 2006). Recent evidence shows that cardiac apoptosis, although at a low level, is present in pressure overload cardiac hypertrophy (Teiger et al., 1996; Li et al., 1997). It has been proposed that chronic low level cardiac myocyte apoptosis may contribute to the pathogenesis of heart failure. In addition to the cardiomyocytes, the TUNEL positive cells that were observed in high percentages in both WT and ATF3^{-/-} (30% v.s. 50%, respectively) after TAB may include both endothelial and interstitial cells, suggesting that ATF3 may play a role in inflammatory signaling.

The precise role of autophagy in the progression of heart failure remains unclear. However, it is possible that autophagic activity performs different functions

MOL #90092

depending on disease staging and severity (Wang et al., 2010). In our ATF3^{-/-} mice with TAB stress, amplification of the autophagic molecule beclin-1 led to abnormal hypertrophic remodeling with early heart failure (Fig. 4B). Our results suggest that enhanced beclin1 activity has pathological consequences, potentially achieved by promoting autophagic cell death or cardiomyocyte necrosis. As beclin-1 has been involved in detrimental autophagic signaling induced by cardiac ischemic/reperfusion injury, our findings further showed that beclin-1, under ATF3 regulation, is involved in cardiac hypertrophic remodeling signaling (Matsui et al., 2007). Beclin-1 can be regulated by microRNA-30a in cancer cells (Zhu et al., 2009). One recent study has demonstrated that the downregulation of microRNA-30a could aggravate pressure overload-induced cardiomyocyte hypertrophy via activating autophagy signaling (Yin et al., 2013). Whether beclin-1 can be repressed by microRNA-30a in heart to attenuate pressure overload-induced cardiac hypertrophy requires further investigation.

In addition to beclin-1, another molecule involved in autophagy, ATG5, was also regulated by ATF3, as indicated by our gel retardation data showing an ATF/CRE binding site located on the upstream promoter region of ATG5 (data not shown). However, ATG5 deletion in the heart resulted in aggravated ventricular enlargement

MOL #90092

and cardiac dysfunction after hemodynamic overload, implying that autophagy induced by ATG5 is a compensatory mechanism during heart failure (Nishida et al., 2008). On the contrary, beclin-1^{+/-} mice subjected to pressure overload have been found to exhibit decreased pathological remodeling and attenuated cardiac dysfunction (Nakai et al., 2007; Zhu et al., 2007). Therefore, it is worth exploring whether ATF3 has a positive or negative influence on the regulation of this conflicting autophagic signaling between ATG5 and beclin-1 in pressure overload-induced heart failure.

ATF3 can be rapidly induced by various stresses, in which Nrf2 can specifically mediate ATF3 induction by acting on the consensus ATF3 response element (ARE) on the ATF3 promoter (Kim et al., 2010; Hoetzenecker et al., 2011). Therefore, for the induction of ATF3 in our experiments, we chose to use the Nrf2 inducer tBHQ. It has been found to have anti-oxidative and anti-inflammatory effects and is used widely as a food preservative (Nishizono et al., 2000; Koh et al., 2009). The administration of tBHQ four weeks after the TAB procedure was found to improve cardiac contractility in mice with prolonged pressure overload-induced heart failure in our study. The beneficial effects offered by tBHQ supplementation may be explained based on both the inhibitory effect of beclin-1-related detrimental autophagy and the inhibitory

MOL #90092

effect on hypertension or angiotensin II-induced cardiac fibrosis and inflammation via the ATF3 pathway. A high dosage of the tBHQ (5 mg/kg), although reported to offer a protective effect on neurons (Koh et al., 2009; Jin et al., 2011), may lead to a high death rate (approximately 50%-70%). Therefore, we used a comparatively low dosage of tBHQ (1 mg/kg) to avoid such severe effects. Recently, several Nrf2 activators including sulforaphane and bardoxolone, and many medicinal plants mixtures (Bai et al., 2013; Reuland et al., 2013; Ruiz et al., 2013), have been reported to protect cardiomyocytes against high glucose or oxidative stress. However, additional studies are required to find out whether consistent results can be obtained from either an ATF3 inducer or an Nrf2 activator after pressure overload-induced heart failure.

In conclusion, our study showed that over-expression of ATF3 or therapy using the ATF3 inducer tBHQ can prevent or rescue cardiac dysfunction induced by pressure overloading by inhibiting beclin-1 associated detrimental autophagic activity. Future therapy using the ATF3 specific inducer tBHQ or other Nrf2 activators may be developed for possible use in the treatment of human chronic hypertension or other pressure overload heart failures.

MOL #90092

Acknowledgements

We thank Ms Pei-Chi King for mouse surgery and mouse husbandry.

Authorship contributions

Participated in research design: Lin, Chen (J.J.), and Cheng

Conducted experiments: Li and Chen (H.H.)

Contributed new reagents or analytic tools: Chen (J.J.), Lai, and Juan

Performed data analysis: Lin, Li, and Cheng

Contributed to the writing of the manuscript: Lin, Li, and Cheng

References

- Bai Y, Cui W, Xin Y, Miao X, Barati MT, Zhang C, Chen Q, Tan Y, Cui T, Zheng Y, and Cai L (2013) Prevention by sulforaphane of diabetic cardiomyopathy is associated with up-regulation of Nrf2 expression and transcription activation. *J Mol Cell Cardiol* 57: 82-95.
- Buganim Y, Kalo E, Brosh R, Besserglick H, Nachmany I, Rais Y, Stambolsky P, Tang X, Milyavsky M, Shats I, Kalis M, Goldfinger N, and Rotter V (2006) Mutant p53 protects cells from 12-O-tetradecanoylphorbol-13-acetate-induced death by attenuating activating transcription factor 3 induction. *Cancer Res* 66: 10750-10759.
- Cao DJ and Hill JA (2011) Titrating autophagy in cardiac plasticity. *Autophagy* 7: 1078-1079.
- Chen BP, Liang G, Whelan J, and Hai T (1994) ATF3 and ATF3 delta Zip, transcriptional repression versus activation by alternatively spliced isoforms. *J Biol Chem* 269: 15819-15826.
- Chen BP, Wolfgang CD, and Hai T (1996) Analysis of ATF3, a transcription factor induced by physiological stresses and modulated by gadd153/Chop10. *Mol Cell Biol* 16: 1157-1168.

MOL #90092

- Dutta D, Calvani R, Bernabei R, Leeuwenburgh C, and Marzetti E (2012) Contribution of impaired mitochondrial autophagy to cardiac aging: mechanisms and therapeutic opportunities. *Circ Res* 110: 1125-1138.
- Erlich S, Mizrachy L, Segev O, Lindenboim L, Zmira O, Adi-Harel S, Hirsch JA, Stein R, Pinkas-Kramarski R (2007) Differential interactions between Beclin 1 and Bcl-2 family members. *Autophagy* 3: 561-568.
- Feihl F, Liaudet L, Levy BI, and Waeber B (2008) Hypertension and microvascular remodelling. *Cardiovasc Res* 78: 274-285.
- Heineke J and Molkentin JD (2006) Regulation of cardiac hypertrophy by intracellular signalling pathways. *Nat Rev Mol Cell Biol* 7: 589-600.
- Hoetzenecker W, Echtenacher B, Guenova E, Hoetzenecker K, Woelbing F, Bruck J, Teske A, Valtcheva N, Fuchs K, Kneilling M, Park JH, Kim KH, Kim KW, Hoffmann P, Krenn C, Hai T, Ghoreschi K, Biedermann T, and Rocken M (2011) ROS-induced ATF3 causes susceptibility to secondary infections during sepsis-associated immunosuppression. *Nat Med* 18: 128-134.
- Hsu JC, Bravo R, and Taub R (1992) Interactions among LRF-1, JunB, c-Jun, and c-Fos define a regulatory program in the G1 phase of liver regeneration. *Mol Cell Biol* 12: 4654-4665.
- Hu P, Zhang D, Swenson L, Chakrabarti G, Abel ED, and Litwin SE (2003)

MOL #90092

Minimally invasive aortic banding in mice: effects of altered cardiomyocyte insulin signaling during pressure overload. *Am J Physiol Heart Circ Physiol* 285: H1261-1269.

Jiang HY, Wek SA, McGrath BC, Lu D, Hai T, Harding HP, Wang X, Ron D, Cavener DR, Wek RC (2004) Activating transcription factor 3 is integral to the eukaryotic initiation factor 2 kinase stress response. *Mol Cell Biol* **24**: 1365-1377.

Jin W, Kong J, Wang H, Wu J, Lu T, Jiang J, Ni H, and Liang W (2011) Protective effect of tert-butylhydroquinone on cerebral inflammatory response following traumatic brain injury in mice. *Injury* 42: 714-718.

Kehat I, Hasin T, and Aronheim A (2006) The role of basic leucine zipper protein-mediated transcription in physiological and pathological myocardial hypertrophy. *Ann N Y Acad Sci* 1080: 97-109.

Kim JY, Lee SH, Song EH, Park YM, Lim JY, Kim DJ, Choi KH, Park SI, Gao B, Kim WH (2009) A critical role of STAT1 in streptozotocin-induced diabetic liver injury in mice: controlled by ATF3. *Cell Signal* **21**: 1758-1767.

Kim KH, Jeong JY, Surh YJ, and Kim KW (2010) Expression of stress-response ATF3 is mediated by Nrf2 in astrocytes. *Nucleic Acids Res* 38: 48-59.

Klionsky DJ and Emr SD (2000) Autophagy as a regulated pathway of cellular

MOL #90092

degradation. *Science* 290: 1717-1721.

Koh K, Cha Y, Kim S, and Kim J (2009) tBHQ inhibits LPS-induced microglial activation via Nrf2-mediated suppression of p38 phosphorylation. *Biochem Biophys Res Commun* 380: 449-453.

Levine B and Klionsky DJ (2004) Development by self-digestion: molecular mechanisms and biological functions of autophagy. *Dev Cell* 6: 463-477.

Li HF, Cheng CF, Liao WJ, Lin H, and Yang RB (2010) ATF3-mediated epigenetic regulation protects against acute kidney injury. *J Am Soc Nephrol* 21: 1003-1013.

Li Z, Bing OH, Long X, Robinson KG, Lakatta EG (1997) Increased cardiomyocyte apoptosis during the transition to heart failure in the spontaneously hypertensive rat. *Am J Physiol* 272: H2313-2319.

Lin H, Cheng CF, Hou HH, Lian WS, Chao YC, Ciou YY, Djoko B, Tsai MT, Cheng CJ, and Yang RB (2008) Disruption of guanylyl cyclase-G protects against acute renal injury. *J Am Soc Nephrol* 19: 339-348.

Ma X, Liu H, Foyil SR, Godar RJ, Weinheimer CJ, Hill JA, and Diwan A (2012) Impaired autophagosome clearance contributes to cardiomyocyte death in ischemia/reperfusion injury. *Circulation* 125: 3170-3181.

Matsui Y, Takagi H, Qu X, Abdellatif M, Sakoda H, Asano T, Levine B, and

MOL #90092

Sadoshima J (2007) Distinct roles of autophagy in the heart during ischemia and reperfusion: roles of AMP-activated protein kinase and Beclin 1 in mediating autophagy. *Circ Res* 100: 914-922.

Nakai A, Yamaguchi O, Takeda T, Higuchi Y, Hikoso S, Taniike M, Omiya S, Mizote I, Matsumura Y, Asahi M, Nishida K, Hori M, Mizushima N, and Otsu K (2007) The role of autophagy in cardiomyocytes in the basal state and in response to hemodynamic stress. *Nat Med* 13: 619-624.

Nishida K, Yamaguchi O, and Otsu K (2008) Crosstalk between autophagy and apoptosis in heart disease. *Circ Res* 103: 343-351.

Nishizono S, Hayami T, Ikeda I, and Imaizumi K (2000) Protection against the diabetogenic effect of feeding tert-butylhydroquinone to rats prior to the administration of streptozotocin. *Biosci Biotechnol Biochem* 64: 1153-1158.

Okamoto Y, Chaves A, Chen J, Kelley R, Jones K, Weed HG, Gardner KL, Gangi L, Yamaguchi M, Klomkleaw W, Nakayama T, Hamlin RL, Carnes C, Altschuld R, Bauer J, and Hai T (2001) Transgenic mice with cardiac-specific expression of activating transcription factor 3, a stress-inducible gene, have conduction abnormalities and contractile dysfunction. *Am J Pathol* 159: 639-650.

Pattingre S, Tassa A, Qu X, Garuti R, Liang XH, Mizushima N, Packer M, Schneider

MOL #90092

MD, Levine B (2005) Bcl-2 antiapoptotic proteins inhibit Beclin 1-dependent autophagy. *Cell* **122**: 927-939.

Rabinowitz JE, Rolling F, Li C, Conrath H, Xiao W, Xiao X, and Samulski RJ (2002) Cross-packaging of a single adeno-associated virus (AAV) type 2 vector genome into multiple AAV serotypes enables transduction with broad specificity. *J Virol* **76**: 791-801.

Reuland D J, Khademi S, Castle CJ, Irwin DC, McCord JM, Miller BF, and Hamilton KL (2013) Upregulation of phase II enzymes through phytochemical activation of Nrf2 protects cardiomyocytes against oxidant stress. *Free Radic Biol Med* **56**: 102-111.

Ruiz S, Pergola PE, Zager RA, and Vaziri ND (2013) Targeting the transcription factor Nrf2 to ameliorate oxidative stress and inflammation in chronic kidney disease. *Kidney Int* **83**: 1029-1041.

St Germain C, O'Brien A, and Dimitroulakos J (2010) Activating Transcription Factor 3 regulates in part the enhanced tumour cell cytotoxicity of the histone deacetylase inhibitor M344 and cisplatin in combination. *Cancer Cell Int* **10**: 32.

Teiger E, Than VD, Richard L, Wisnewsky C, Tea BS, Gaboury L, et al (1996) Apoptosis in pressure overload induced heart hypertrophy in the rat. *J Clin*

MOL #90092

Invest 97: 2891–2897.

von Harsdorf R, Edwards JG, Shen YT, Kudej RK, Dietz R, Leinwand LA,

Nadal-Ginard B, and Vatner SF (1997) Identification of a cis-acting regulatory element conferring inducibility of the atrial natriuretic factor gene in acute pressure overload. *J Clin Invest* 100: 1294-1304.

Wang A, Arantes S, Yan L, Kiguchi K, McArthur MJ, Sahin A, Thames HD, Aldaz

CM, Macleod MC (2008) The transcription factor ATF3 acts as an oncogene in mouse mammary tumorigenesis. *BMC Cancer* 22: 268.

Wang Z, Zhu T, Qiao C, Zhou L, Wang B, Zhang J, Chen C, Li J, and Xiao X (2005)

Adeno-associated virus serotype 8 efficiently delivers genes to muscle and heart. *Nat Biotechnol* 23: 321-328.

Wang ZV, Rothermel BA, and Hill JA (2010) Autophagy in hypertensive heart

disease. *J Biol Chem* 285: 8509-8514.

Xiao X, Li J, and Samulski RJ (1998) Production of high-titer recombinant

adeno-associated virus vectors in the absence of helper adenovirus. *J Virol* 72: 2224-2232.

Yin X, Peng C, Ning W, Li C, Ren Z, Zhang J, Gao H, Zhao K (2013) miR-30a

downregulation aggravates pressure overload-induced cardiomyocyte hypertrophy. *Mol Cell Biochem* 379: 1-6.

MOL #90092

Yorimitsu T and Klionsky DJ (2005) Autophagy: molecular machinery for self-eating.

Cell Death Differ 12 Suppl 2: 1542-1552.

Zhou H, Shen DF, Bian ZY, Zong J, Deng W, Zhang Y, Guo YY, Li H, and Tang QZ

(2011) Activating transcription factor 3 deficiency promotes cardiac hypertrophy, dysfunction, and fibrosis induced by pressure overload. *PLoS*

One 6: e26744.

Zhu H, Tannous P, Johnstone JL, Kong Y, Shelton JM, Richardson JA, Le V, Levine

B, Rothermel BA, and Hill JA (2007) Cardiac autophagy is a maladaptive response to hemodynamic stress. *J Clin Invest* 117: 1782-1793.

Zhu H, Wu H, Liu X, Li B, Chen Y, Ren X, Liu CG, Yang JM (2009) Regulation of

autophagy by a beclin 1-targeted microRNA, miR-30a, in cancer cells.

Autophagy 5: 816-823.

MOL #90092

Footnotes

H.L. and H-F.L. contributed equally to this work.

Financial support: This work was supported by grants from the National Science Council, Taiwan [98-2314-B-320-003] and the Department of Health, Executive Yuan, Taiwan [DOH101-TD-PB-111-NSC013] to Heng Lin., and from Tzu Chi General Hospital [TCRD101-10 and TCRD102-17] and Tzu Chi University [TCIRP 99001 and TCIRP102001] to Ching-Feng Cheng.

Conflict of interest: none declared

Figure Legends

Fig. 1. Increased ATF3 expression was found in the heart of cardiac hypertrophic mice induced by transverse aortic banding (TAB). (A) Quantitative RT-PCR analysis, * indicates $P < 0.05$. (B) Immuno-histochemical analysis of cardiac ATF3 expression in the sham- and TAB mice (n=5 for each group). Arrows indicate translocation of ATF3 into the nucleus. (C) Translocation of ATF3 was confirmed by Western blot analysis. Nuclear and cytosolic extracts were probed with specific antibody against ATF3. Anti- β -actin and anti-Lamin A/C served as a loading control.

Fig. 2. Loss of normal cardiac hypertrophic remodeling with increased fibrosis and apoptosis in TAB treated ATF3^{-/-} mice. (A) Real-time RT-PCR analysis on cardiac tissue for hypertrophic markers α -MHC (myosin heavy chain), β -MHC, ANF (atrial natriuretic factor), and BNP (brain natriuretic peptide) at 2 weeks after TAB treatment (n=5 for each group). The mean normalized value for the expression of each gene in sham-operated hearts is defined as 1. * indicates $P < 0.05$ (B) Masson's trichrome staining for cross-sectioned heart and morphometric quantitation of fibrosis area were shown on both wild type (WT) and ATF3^{-/-} mice subjected to TAB treatment. Bar=2 mm. * indicates $P < 0.05$. Data reflect measurements from at least 4

MOL #90092

animals per group. (C) Detection of apoptotic heart cells using *in situ* TUNEL staining. Diagram for the TUNEL positive cells represent data from five independent experiments; Bar=100 μ m; * indicates $P < 0.05$. (D) A representative expression of cleaved, active caspase-3 in the WT and ATF3^{-/-} mice was shown. Experiments were repeated for 2 times with similar results.

Fig.3. Recovery of left ventricular contractility and attenuation of cardiac fibrosis in TAB-treated ATF3^{-/-} mice after AAV8-ATF3 therapy. (A) Western blot of cardiac ATF3 expression in ATF3^{-/-} mice with or without AAV-ATF3 injection. (B) Echocardiographic measurements were performed at 3 weeks after TAB procedures in WT and ATF3^{-/-} mice with or without AAV-ATF3 therapy. EF, ejection fraction ; FS, fraction shortening. (C) Masson's trichrome staining of cross-sectioned heart and morphometric quantitation of fibrosis area in WT and ATF3^{-/-} mice with or without AAV-ATF3 therapy; Bar= 2 mm.

Fig. 4. ATF3 inhibited autophagy by a beclin-1 dependent pathway. (A) Protein level of beclin-1 was inhibited by adenovirus-induced ATF3 (Adv-ATF3) overexpression in H9c2 cells under starvation conditions. (B) Western analysis of beclin-1 in WT and ATF3^{-/-} mice after TAB. (C) The protein expression of LC3B in

MOL #90092

WT and ATF3^{-/-} mice after TAB was confirmed by Western blot analysis. Anti-GAPDH served as a loading control. (D) Binding activity of ATF3 on the ATF/CRE binding site of beclin promoter. Results of EMSA with the ATF/CRE probe in the nuclear extracts of in vitro transcription translation and in the presence of 100X concentration of unlabeled competitor probe (cold probe). (E) Chromatin was isolated from Adv-ATF3-treated or untreated H9c2 cells. Chromatin immunoprecipitation (ChIP) experiments were carried out with ATF3-specific antibody and primers to amplify -164 to -156 of the beclin locus, which contained one predicted ATF/CRE binding site in mouse. The data are representative of 2-4 independent experiments. (F) ATF3 suppressed beclin-1 promoter activity through ATF/CRE binding site in 293T cells which were transiently co-transfected with indicated plasmids. Cells were collected and assayed for luciferase activity in both stress (starvation) and non-stress condition; * indicates P < 0.05. (G) Luciferase activity on PGL4-beclin promoter expression in heart tissue of both WT and ATF3^{-/-} mice 3 days after TAB treatment.

Fig 5. Treatment with ATF3 activator tert-butylhydroquinone (tBHQ) attenuated TAB-induced LV dilatation and increased contractility in mice. (A) Real time PCR analysis on cardiac ATF3 expression at 1 day or 7 day after different dosages of

MOL #90092

tBHQ therapy. (B) Experimental timeline for TAB and tBHQ therapy. Mice were treated with i.p. tBHQ (1 mg/kg) weekly from 4 to 10 weeks after TAB procedure. (C) Echocardiographic measurements were performed on mice before (week 4) and after (week 10) tBHQ therapy in both TAB-procedure group and non-procedure group. Parameters including inter-ventricular septum thickness at diastole (IVSd) and systole (IVSs), left ventricular internal diameter at diastole (LVIDd) and systole (LVIDs), left ventricular posterior wall thickness at diastole (LVPWd) and systole (LVPWs), fractional shortening of left ventricle (FS), ejection fraction of left ventricle (EF), and heart rate (HR) were shown; * indicates $P < 0.05$.

Fig 6. Therapy using ATF3 activator tert-butylhydroquinone (tBHQ) attenuated TAB-induced apoptosis in mice. *In situ* TUNEL staining of heart cells in WT mice following sham operation or TAB injury with or without tBHQ treatment. Diagram for the TUNEL positive cells represent data from five independent experiments; Bar=200 μm ; * indicates $P < 0.05$.

Table 1 Primers used

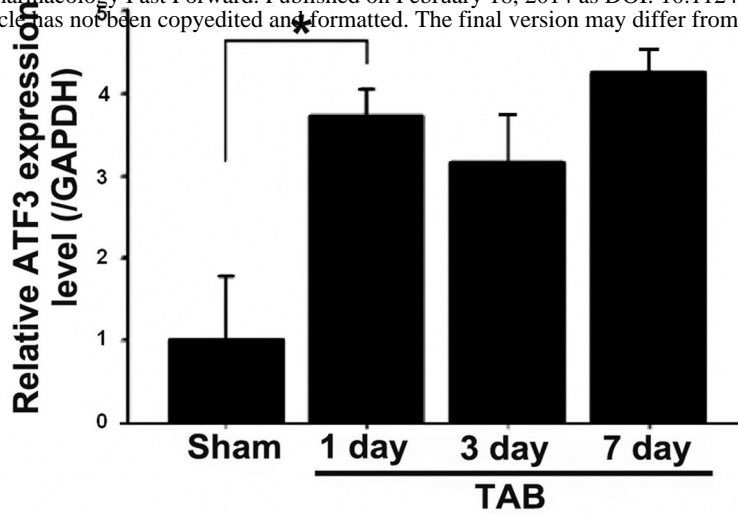
Gene	Forward	Reverse	Assay
mATF3	TTGGATCCATGATGCTTCAA CAC	CCCAAGCTTTTACTTGTCATC GTC	Q-PCR
GAPDH	GGAGCCAAACGGGTCATCA TCTC	GAGGGGCCATCCACAGTCTT CT	Q-PCR
m α -MHC	AGAAGCCCAGCGCTCCCTC A	TGCCTCGGGTCAGCTGGGAA	Q-PCR
m β -MHC	AACCTGTCCAAGTTCCGCA AGGTG	GAGCTGGGTAGCACAAGAG CTACT	Q-PCR
mANF	CTCCGATAGATCTGCCCTCT TGAA	GGTACCGGAAGCTGTTGCAG CCTA	Q-PCR
mBNP	GCTCTTGAAGGACCAAGGC CTCAC	GATCCGATCCGGTCTATCTTG TGC	Q-PCR
mbecln(\square 182)	CAGGGGTCCTTGCGTCAGC TCCCGTC	GACGGGAGCTGACGCAAGG ACCCCTG	EMSA
mbecln(\square 164)	CTCCCGTCGTGACGTCACT TCTGGTC	GACCAGAAGTGACGTCACG ACGGGAG	EMSA
beclin-1 promoter	CCGCTCGGCCTTTGGATGG C	ACCCAGGCTCGTTCTACCGC	CHIP

h, human; m, mouse; Q-PCR, quantitative PCR.

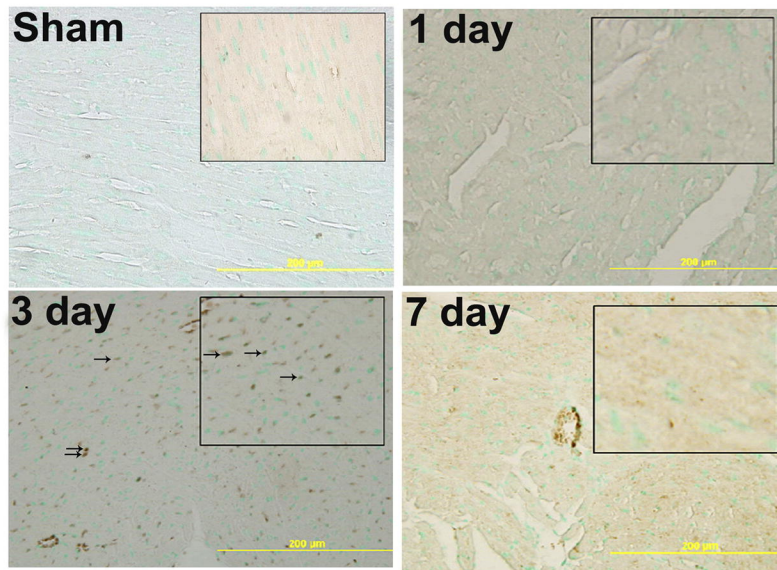
Fig. 1

A

Molecular Pharmacology Fast Forward. Published on February 18, 2014 as DOI: 10.1124/mol.113.090092
This article has not been copyedited and formatted. The final version may differ from this version.



B



C

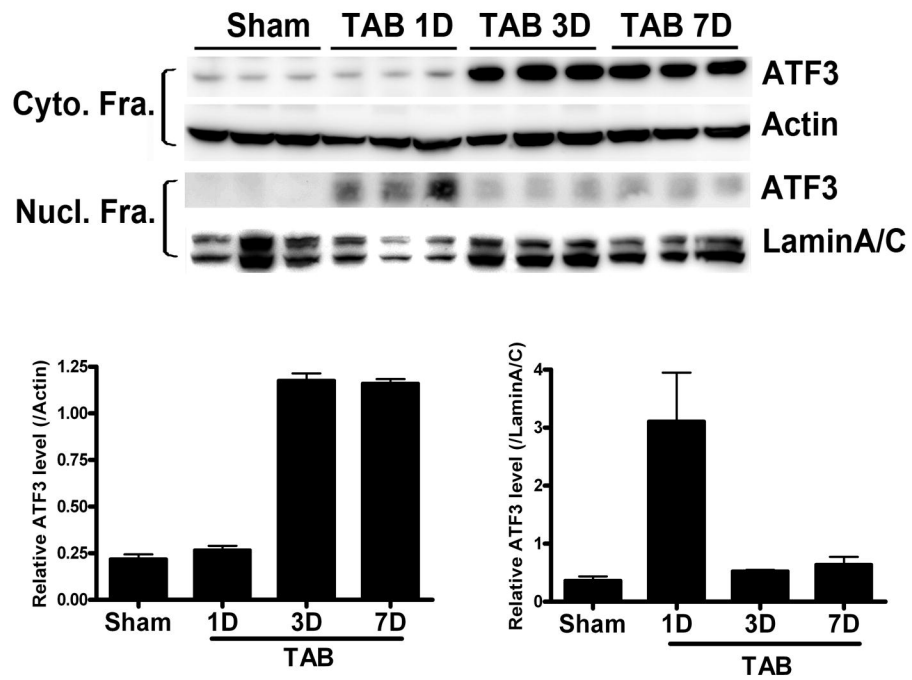


Fig. 2

Molecular Pharmacology Fast Forward. Published on February 18, 2014 as DOI: 10.1124/mol.113.090092
This article has not been copyedited and formatted. The final version may differ from this version.

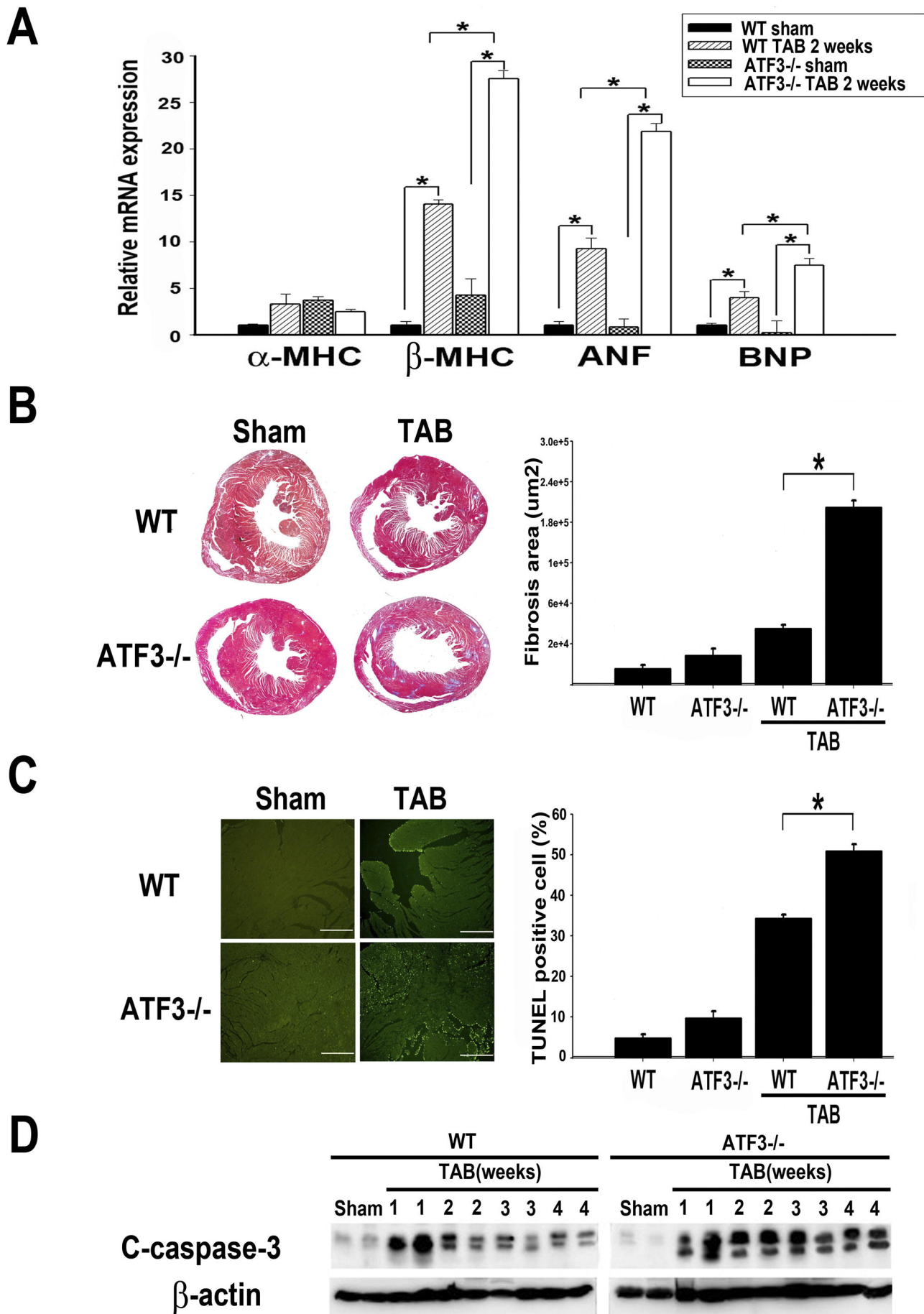
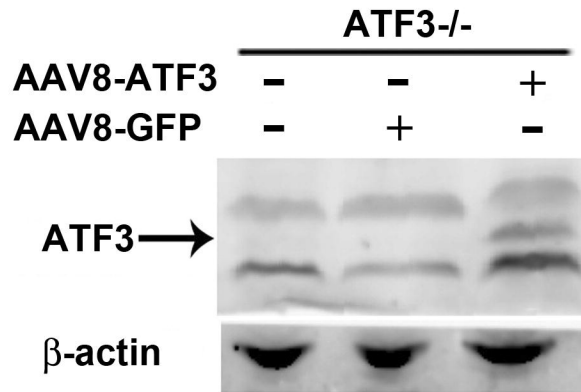


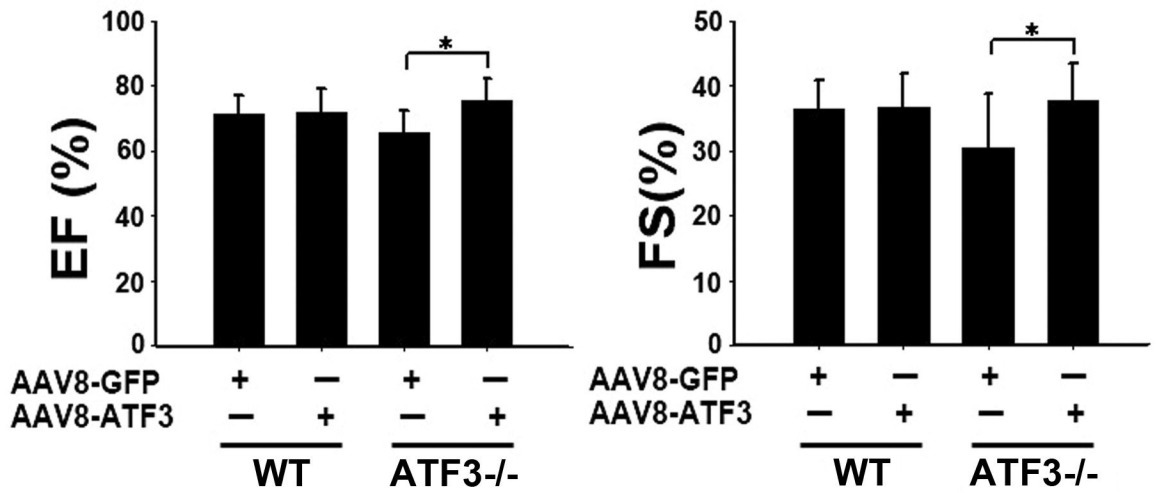
Fig. 3

Molecular Pharmacology Fast Forward. Published on February 18, 2014 as DOI: 10.1124/mol.113.090092
 This article has not been copyedited and formatted. The final version may differ from this version.

A



B



C

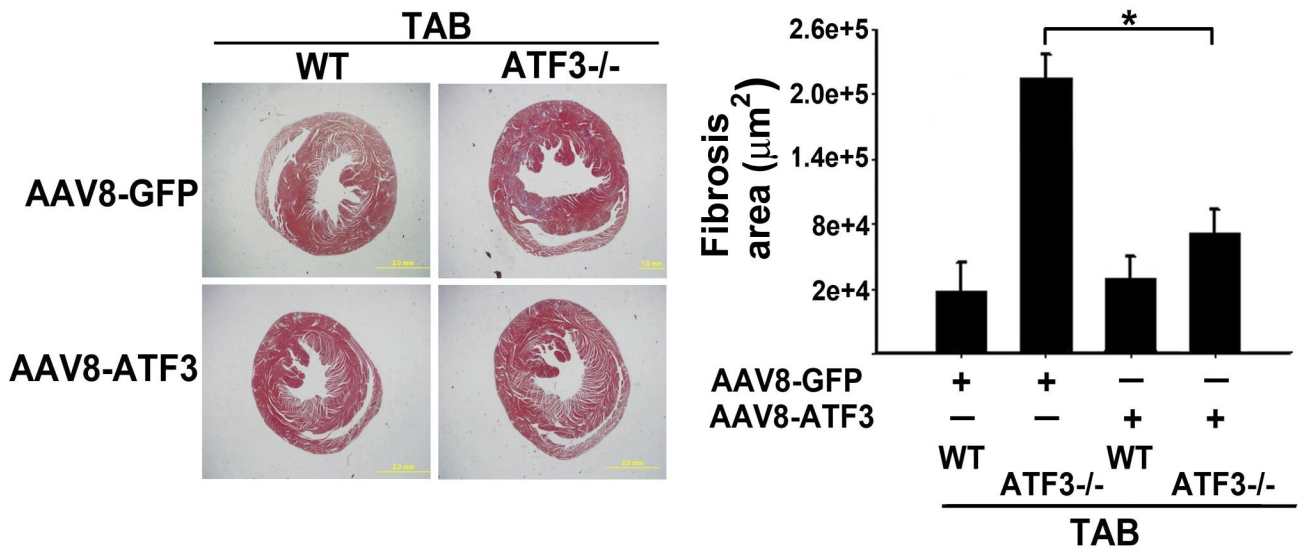
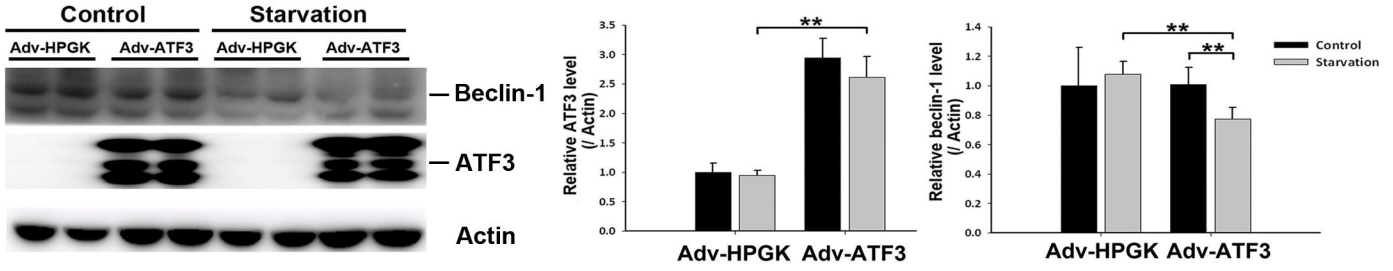


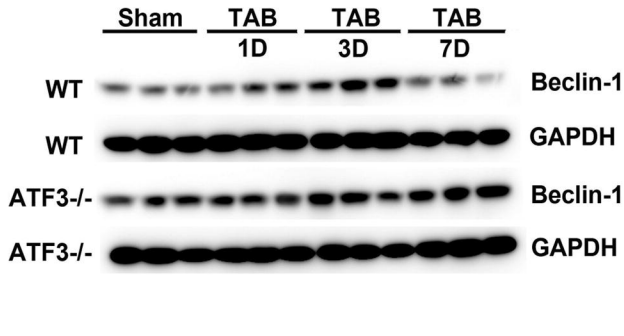
Fig. 4

Molecular Pharmacology Fast Forward. Published on February 18, 2014 as DOI: 10.1124/mol.113.090092
This article has not been copyedited and formatted. The final version may differ from this version.

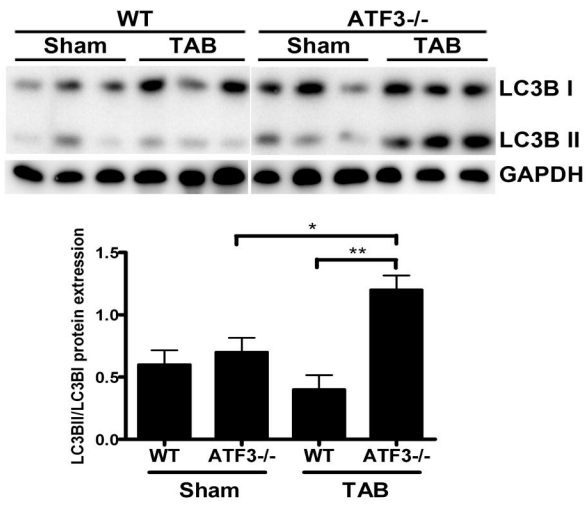
A



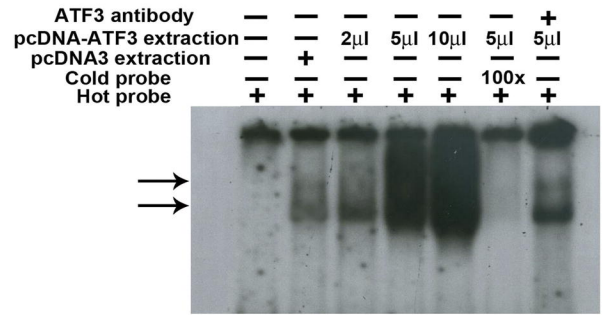
B



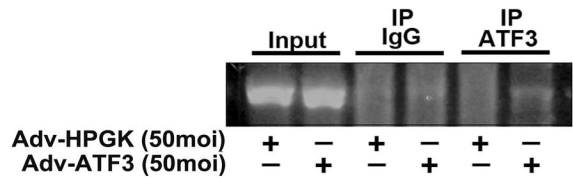
C



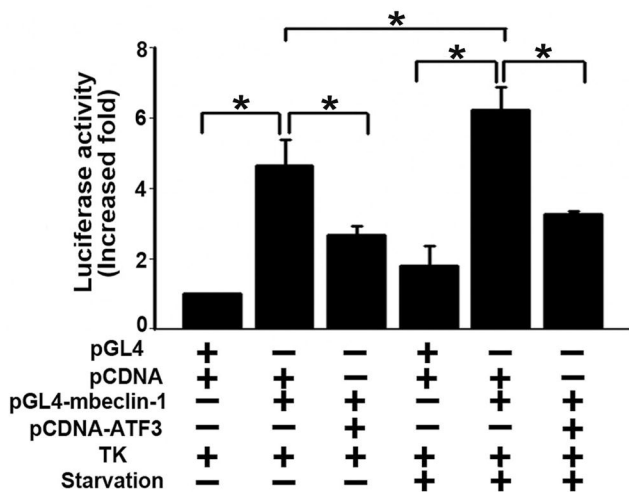
D



E



F



G

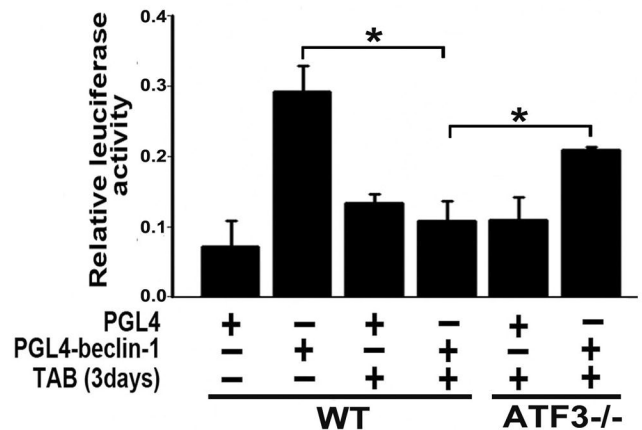
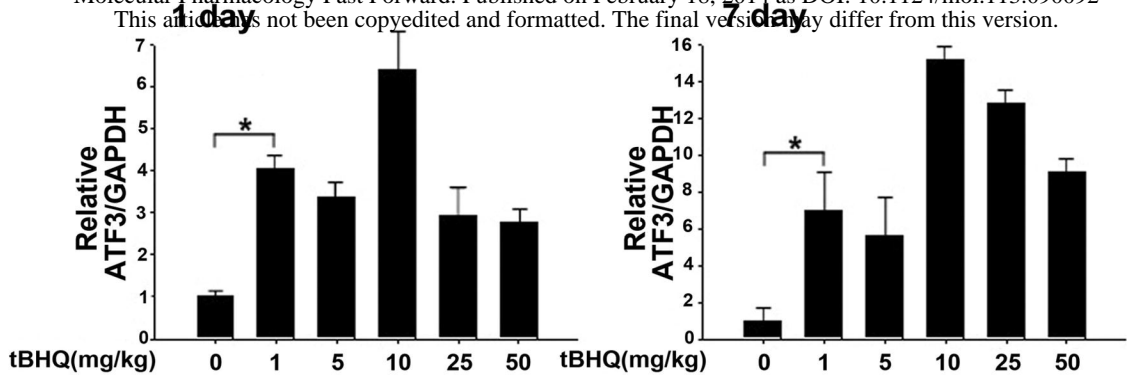


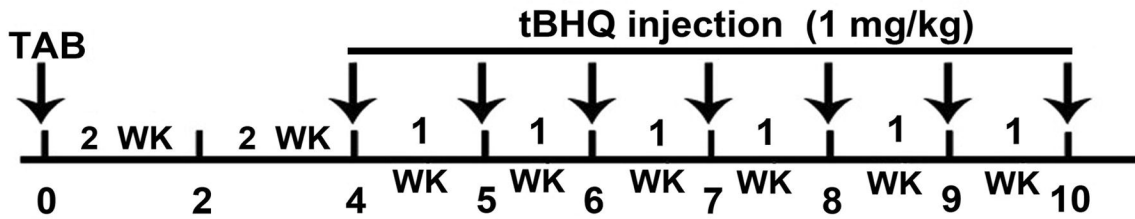
Fig.5

Molecular Pharmacology Fast Forward. Published on February 18, 2014 as DOI: 10.1124/mol.113.090092
 This article has not been certified by peer review and should not be used to guide clinical practice.

A



B



C

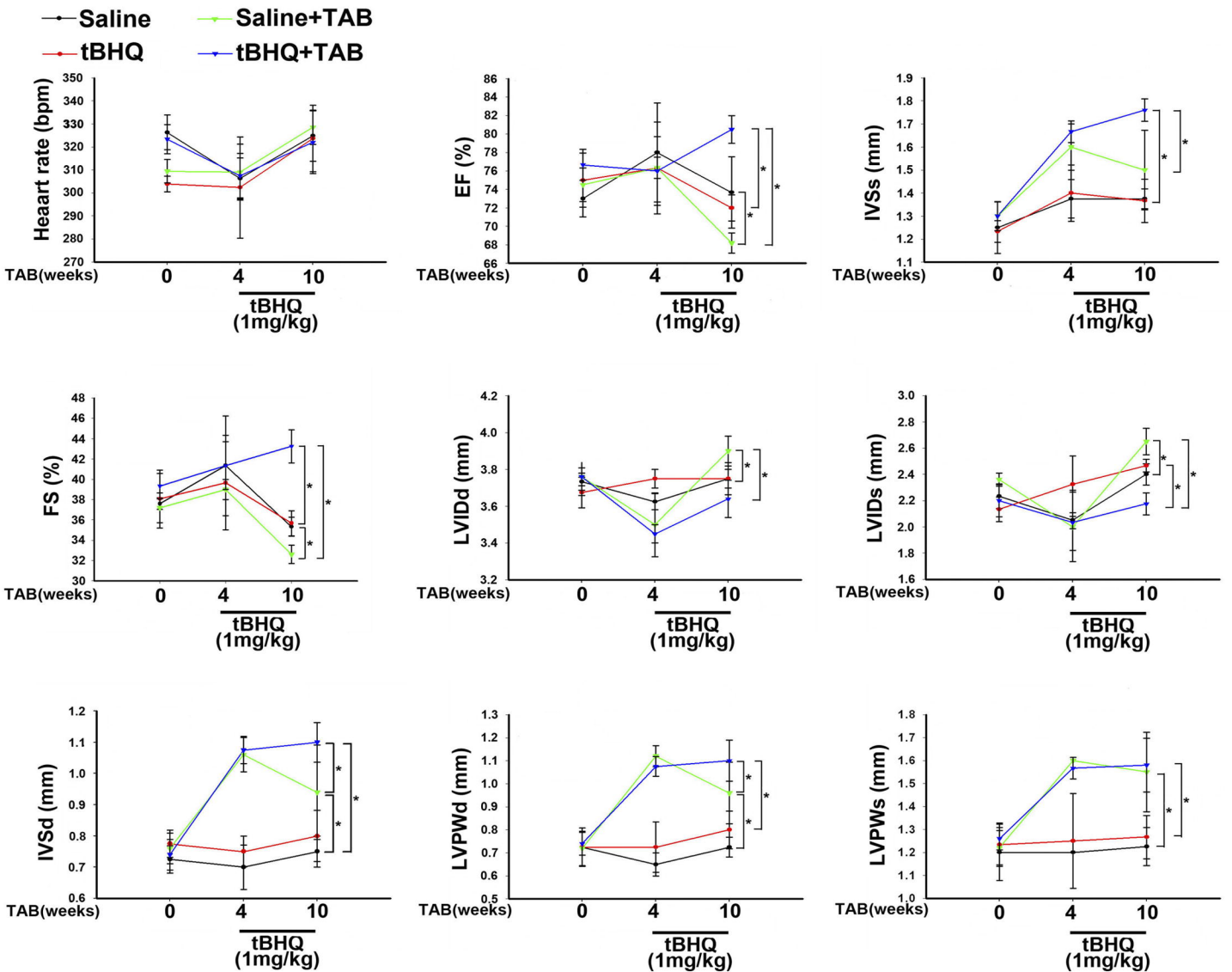


Fig. 6 Molecular Pharmacology Fast Forward. Published on February 18, 2014 as DOI: 10.1124/mol.113.090092
This article has not been copyedited and formatted. The final version may differ from this version.

